Expecting and comparing palmprint features using Radon transform and Sparse representation

Major Project Report submitted in partial fulfillment of the rewards requirements for the award of degree of

Master of Technology

in

Information Systems

Submitted By:

Deepika Vatsa

(2k11/ISY/05)

Under the Guidance of:

Sh. Anil Singh Parihar

(Assistant professor, IT Department)

Department of Information Technology
Delhi Technological University
Bawana Road, Delhi – 110042

(2011-2013)

CERTIFICATE

This is to certify that **Ms. Deepika Vatsa** (2k11/ISY/05) has carried out the major project titled "**Expecting and comparing palmprint features using Radon transform and Sparse representation**" as a partial requirement for the award of Master of Technology degree in Information Systems by Delhi Technological University.

The major project is a bonafide piece of work carried out and completed under my supervision and guidance during the academic session 2011-2013. The matter contained in this report has not been submitted elsewhere for the award of any other degree.

(Project Guide)

Sh. Anil Singh Parihar

Assistant professor, Department of Information Technology

Delhi Technological University

Bawana Road, Delhi-110042

ACKNOWLEDGEMENT

I express my deepest gratitude towards my guide **Sh. Anil Singh Parihar** for his constant help and encouragement throughout the project work. I have been fortunate to have a guide who gave me the freedom to explore on my own and at the same time helped me plan the project with timely reviews and suggestions wherever required. This thesis could not have been written without his unending and enthusiastic support. It is my pleasure to record my sincere thanks to my respected guide.

I humbly extend my words of gratitude to **Sh. O. P. Verma**, Head of Department and other faculty members of this department for providing their invaluable help and time whenever it was required.

Deepika Vatsa
Roll No. 2k11/ISY/05
M.Tech (Information Systems)
E-mail: vatsa.deepika@gmail.com

Abstract

Palmprint is the most widely used biometric identifier for personal identification. However, work on principal lines of palmprint is less due to the similarity of principal lines in different individuals. This paper investigates a new approach utilizing the capabilities of sparse representation and radon transform to improve the recognition and verification problems. Gabor filter is used to highlight the textural features in the palmprint which further enhances the performance. In this work, ease of computation of radon transform is exploited while a solution for sparse representation of radon transform orientation dictionary using convex optimization approach. We perform experiments on two publicly available PolyU and IITD palmprint databases and the results were recorded from both the approaches i.e. Radon transform and sparse representation based on radon transform. A significant improvement is observed in case of sparse representation based on radon transform technique than just applying radon transform, thus confirms the practical importance of this approach in real life palmprint identification problems. Since sparse representation based on radon transform outperforms radon transform technique, this approach is also applied on PolyU Knuckleprint database and the results were recorded.

Table of Contents

List of Figures

List of Tables

Chapter 1
Introduction

1.1 Biometrics and Security

Biometrics is any quantifiable characteristic of human which has the ability to uniquely identify that person. Biometrics was introduced in 1970s and early 1980s. At that time , it was used to identify people on the basis of unique physical characteristics like scars, height, complexion etc . In ancient china, it was employed to distinguish on the basis of their ink stamped palmprints. Later in 1990s, its applicability shifted greatly towards criminology thus detecting criminal tendencies. Currently biometrics is employed in security processes since they are used in prison visitor system, online payment systems, bank vaults etc. where fraud is a risk.

In today's society, where technology and innovation is getting better every minute and crime has become a common event, there is an increase demand of security to compete with the new fraud challenges. It calls for new and efficient authentication techniques to compete with potential fraud schemes. Biometrics greatly helps in security operations and found much better in performance than the traditional resources of security.

Today, existing Authentication techniques are:

1. Possession-based
2. Knowledge-based
3. Physiology-based

Possession-based authentication technique means something only the concerned individual possesses such as keys, tokens, smart cards etc.
Knowledge-based authentication technique means something only the concerned individual knows such as PIN number, answer of security question, password etc.

Physiology-based authentication technique means something only the concerned individual has. This is where biometrics comes into picture.
These techniques are shown in figure 1.1.

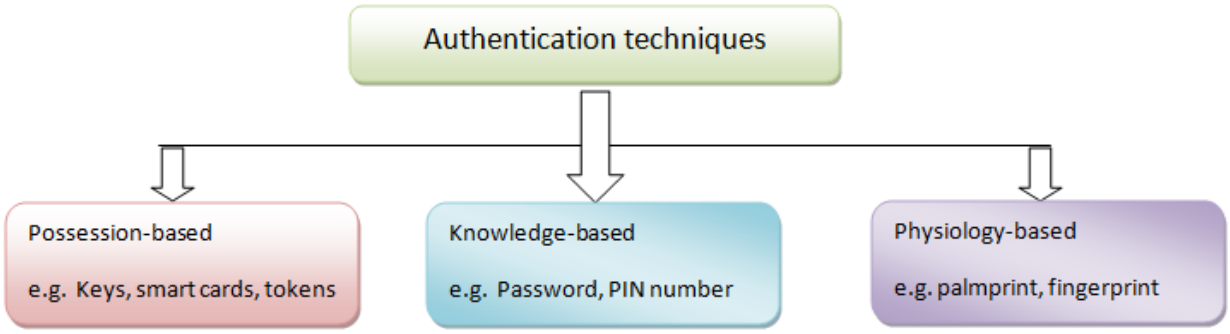

Fig. 1.1 Different authentication techniques.

Out of these, possession–based and knowledge-based techniques are traditional techniques of security while physiology-based technique refers to biometrics.

Over possession-based and knowledge-based techniques, physiology-based technique has its own importance and advantages. In possession-based techniques, there is an overhead of carrying keys, tokens, smart cards plus the risk of dropping them mistakenly. In knowledge-based techniques, one needs to remember the password or the PIN number. Also, passwords can be easily guessed or compromised since many users choose easy passwords for their accounts so they could not forget them. With little effort, they can be guessed and thus the account can easily be cracked. In physiology-based techniques, concerned person need not carry anything or remember anything for security issues, like in knowledge-based and possession-based techniques. There is no risk of keys or tokens being stolen. There is no overhead of remembering so many passwords. Biometrics relieves the person from all these overheads as biometrics can never be stolen or compromised.

Thus biometrics offers great advantages over traditional methods:

1. Increased security as no fraud scheme can be planned and executed

2. Increased convenience as user need not carry anything or remember anything.
3. Increased accountability as they protect individual's privacy.
4. Reduce risk of financial losses to organizations.

Benefits of biometrics in security systems:

1. Fraud detection: It greatly helps in fraud detection by identifying and verifying individuals. Biometrics characteristics are difficult to fake or change on purpose. Also no hacking method can do anything.
2. Fraud deterrence: With the risk of being caught, people don't dare to challenge security system thus maintaining security and ensuring privacy. Thus it stops people to commit crime, which is a great success in itself.
3. Biometrics are suitable for large scale organizations as well since even if there are thousands of millions of employees, identifying these much number of employees would not be a problem with biometrics system but password setting for these many employees could be a problem.

1.2 Background

1.2.1 Biometrics

Biometrics explains itself as it is a combination of two words: bio and metrics. Bio means biological traits/modalities and metrics means statistics. So, biometrics is a branch of science which deals with measurable biological traits and observes them using statistical analysis and thus helps in personal identification.

1.2.2 Biometric systems

Biometric system is basically a pattern recognition system that first acquires biometric data from an individual, extract feature set from the acquired data and then compare this feature set against the template set(previously acquired and stored) in the database.

Biometrics systems perform recognition to accurately recognize individuals based on their physiological or behavioral traits. Biometric systems operate in two modes:

1. Verification mode: In verification mode, the biometric system verifies the individual's identity by comparing his captured biometric data and his own biometric template enrolled and stored in database. So system conducts a one-to-one comparison determining whether the claim is true or false.

2. Identification mode: In identification mode, the system recognizes an individual by performing one-to-many comparisons with the templates of all the users stored in the database.

Block diagram of these modes is shown in figure 1.2.

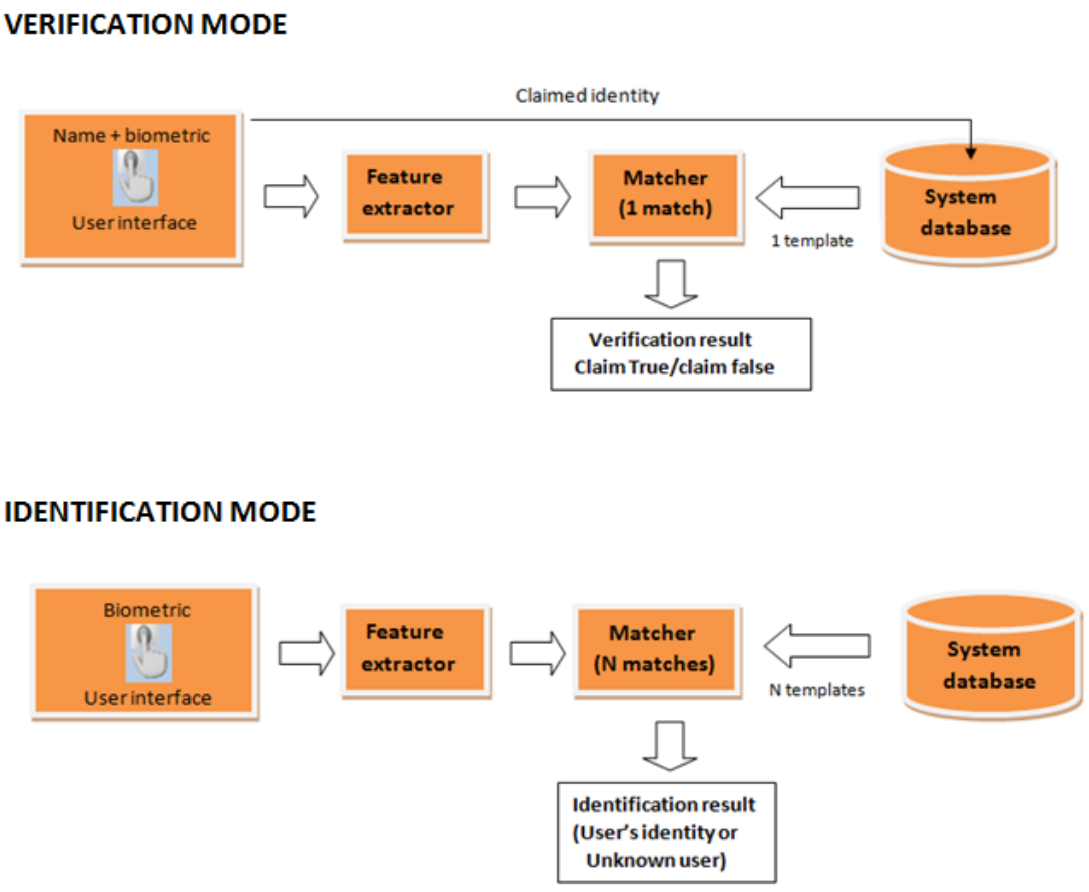

Fig. 1.2 Block diagram of verification mode and identification mode

A biometric system has following four main components:-

1. Sensor: It is one of the important components of biometric system which helps in acquiring biometric data from an individual.

2. Feature extraction component: This component process and analyze the acquired data to extract a set of invariable features from them which helps in uniquely identifying an individual. It generates a expressive and compact representation called template. For e.g., position and orientation of minutiae points in a fingerprint image are extracted from the acquired fingerprint image. Then the orientation information of all the minutiae points will be called a template.

3. Matcher component: It is the fundamental component of biometric system. It compares the extracted features against the stored feature templates and generates a matching score. A decision function is inbuilt in the matcher component which on the basis of matching score either confirms a user's identity (verification systems) or establishes it (identification systems) depending on the mode of biometric system. Decision function takes into account the matching score and the threshold value to make a decision. Matching score is a value on a scale of low to high which measures the success of match. The threshold value is a benchmark score above which the match between the stored biometric and the individual is considered acceptable or below which it is considered unacceptable.

4. System database component: This component is used to store the templates of enrolled users. The database should be large enough to hold a decent number of templates.

The biometric systems are capable of processing and comparing thousands of entries in a second. The matching ability of a biometric system can never be 100 percent; it only gives a statistical probability. Even two samples from the same user do not match perfectly because of various factors: noisy sensor input, ambient conditions, imperfect

imaging conditions, cuts, bruises etc. Two rates measure the authentication ability of a biometric system:

1. False match rate (FMR): It is the percentage of incorrect matches. That is biometric system in this case mistaken two biometric templates of different persons as of same person. It is also known as false acceptance rate. False match rate can be calculated as:

$$FMR = \frac{Total\ False\ Matches}{Total\ False\ Attempts}$$

2. False non-match rate (FNMR): It is the percentage of incorrect non-matches or valid matches being rejected [2]. That is biometric system in this case mistaken two biometric templates of same person as of different persons. It is also known as false rejection rate. False non match rate can be calculated as:

$$FNMR = \frac{Total\ False\ NonMatches}{Total\ True\ Attempts}$$

These two rates measure the accuracy of a biometric system. There is a tradeoff between false match rate and false non-match rate in every biometric system either to increase security or convenience. Both are function of threshold.

- If threshold is decreased to make the application more convenient to users, many impostors can have access to the application i.e. FMR increases.
- On the other hand, if threshold is increased to make the application more secure, many genuine people may get rejected to use the application, then FMR decreases but FNMR increases.

This tradeoff between security and convenience can be represented by a receiver operating characteristic (ROC) curve. A ROC curve is a plot of FMR and FNMR for

various threshold values with FMR on vertical axis and FNMR on horizontal axis [2].

Depending on the application, a ROC plot can be plotted as in figure 1.3 shown below.

High security applications usually set a very high threshold value, to prevent invalid users to have access to the application. The operator might even afford to reject some valid users, only to be sure no access is granted to invalid users. Forensic applications, on the other hand, set a lower threshold. Here, the forensic operator might accept to inspect a greater number of incorrect matches. Civilian applications set a mediocre threshold value keeping in mind both security and convenience.

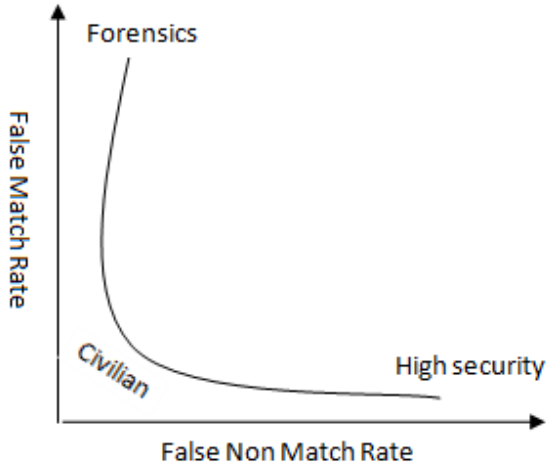

Fig. 1.3 Receiver operating characteristic curve of a biometric system

Applications of Biometrics:

1. Forensic applications like in criminal case investigations or terrorist identification, missing children, DNA matching etc.
2. Government applications, including use in civil and military areas, aadhar card etc.
3. Commercial applications, including account logins; physical access control, ATM

PIN entry; credit cards etc.

4. Other applications, like car park surveillance etc.

1.2.3 Traits and their Features

Traits are the characteristics of human which help identify an individual. The presence of following characteristics enable the biological traits to become a biometric trait:

1. Universality: Trait should be possessed by each and every individual.
2. Collectability: Trait should be quantitatively measurable.
3. Distinctiveness: Trait should exhibit different features in different individuals so that each individual's trait is unique to them.
4. Permanence: Traits should be invariant with time.
5. Acceptability: Trait should be acceptable by population that will use the biometric system.

Biological traits can be of two types:

1. Physiological traits: They are stable human characteristics such as fingerprints, pattern of veins, face geometry, hand geometry, palmprint etc. They are passive traits as they do not change with time.

2. Behavioral traits: These are the human characteristics which are exhibited by the behavior of a human or by the functions he performs such as gait movement, voice, signature dynamics etc. They are active traits.

Features of an image are the information which can uniquely characterize that image. In many biometric applications, input image of the suitable modality is taken which is first preprocessed and then features are extracted which uniquely represent the identity of the person. Features are some quantifiable measures of the image like texture, orientation etc.

Features should be scale and rotation invariant. These features are described by feature vectors also called feature descriptors. These features then help in classification task.

1.3 Introduction to palmprint and knuckleprint

1.3.1 Palmprint

Palmprint is the image of the inner surface of the palm region of the hand. Palmprint is the widely used biometric trait after fingerprint which is in use from ancient times. Palmprints are unique and difficult to fake thus making it a suitable biometric for many security applications. Palmprint is a highly accurate biometric trait for feature extraction as it provides a greater surface area for distinctive feature extraction. Palmprint has grabbed the attention of many researchers because abundant number of features can be retrieved from the palmprint. One can gain following information from the palmprint image: palm geometry (palm area, palm width, palm length), principal lines structure, principal lines orientation, wrinkles (secondary lines) structure and orientation, point features (ridges) and texture information. Palmprint differs to a fingerprint as fingerprint does not contains other information such as texture, wrinkles, line alignments which can be used when comparing one palm to another. Thus, palmprint is a better trait to be use as biometric to compensate for insufficiency of fingerprint in providing valuable and distinct features. Other advantages of palmprint over traditional fingerprint includes: low cost of palmprint capturing device and less memory requirements as palm images are low resolution images.

In a palmprint, there are three principal lines namely life line, heart line and head line (refer figure 1.4 [6]). They remain stable and cannot be counterfeited. By intersecting the principal lines from two sides of the palm, we get two points *a* and *b* and one intersecting point *o*. These points *a, b* and midpoint *o* remains unchanged for long time (years). These points are rotation invariant thus can be treated as features while comparing two palm

images. Palm can also be divided into three regions namely: finger-root region, inside region and outside region [6].

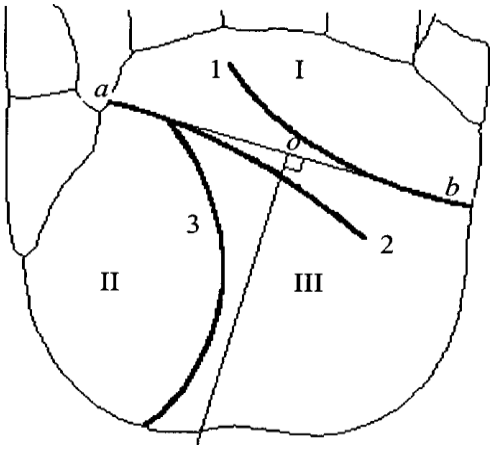

Fig. 1.4 Palmprint image: principal lines (1, heart line; 2, head line; 3, life line), regions (I, finger-root region; II, inside region; III, outside region), end points (a and b), and their midpoint (o)[6].

In palmprint authentication technique, features are not extracted directly from the image taken at the interface. There are few steps needed to be done prior to feature extraction:

1. Image acquisition
2. Preprocessing
3. ROI extraction

1. Image acquisition: For image acquisition, the acquisition device include the following tools: a ring source, CCD camera, lens, frame grabber and A/D converter [7]. Figure 1.5 illustrates the diagrammatic representation of steps taken during acquisition. The ring source enables proper lightning condition during capturing of image. CCD camera captures the image and sends it to A/D convertor which converts the image into digital image which is then stored in computer.

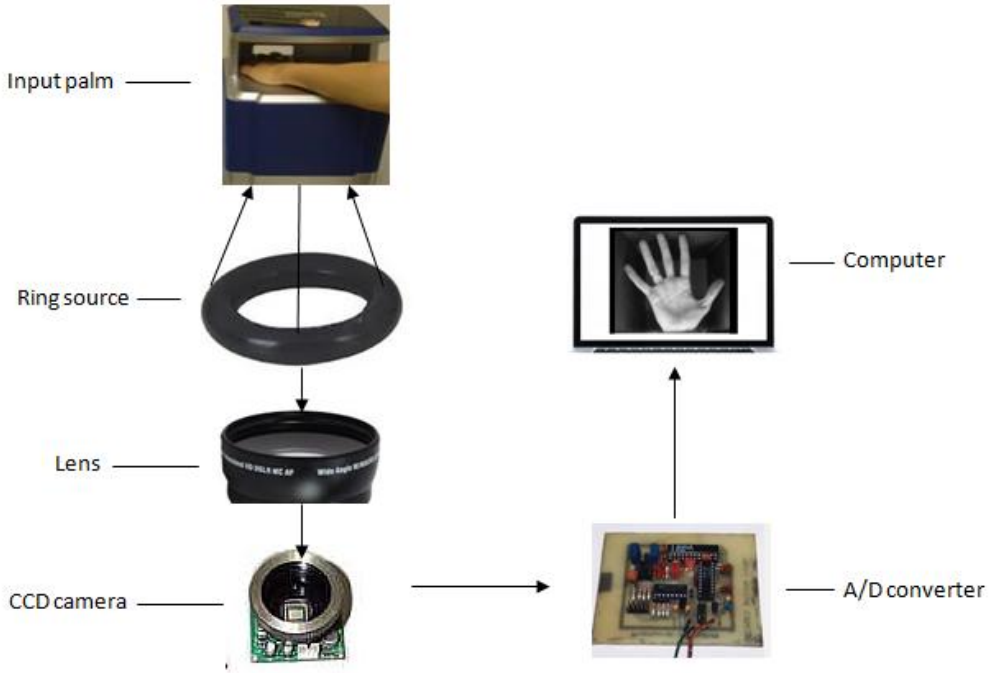

Fig. 1.5 Palmprint acquisition system

2. Preprocessing: The digital palm image taken is first preprocessed so that it becomes efficient for feature extraction because performance of feature extraction techniques is directly affected by the quality of input image. So in preprocessing step, image is enhanced so that reliable and efficient features could be extracted. Goal of preprocessing step is to remove noise, improve clarity of image, remove sharpness etc.

3. Palm ROI extraction: ROI stands for Region of Interest. Before extracting features we have to extract a selected portion of palm image from where we will extract features. Original palm image and its extracted ROI are shown in figure 1.6.

   In ROI extraction phase, the preprocessed palm image is first convolved with the Gaussian filter to smoothen the image. Then the resultant image is binarised using a suitable threshold. Then the boundary of this binarised image is achieved using boundary tracking algorithm. Gaps between the fingers in the palm image play the

major role in extracting ROI of palm image. However a boundary of the gap between middle finger and ring finger is not extracted. So we achieved two gaps, one from middle finger and index finger & one from ring finger and little finger. Draw a tangent joining these two points (gaps). Then from the midpoint of the line joining these two points, draw a perpendicular till it reaches the boundary on other side to determine the origin of the coordinate system. Then extract a region of suitable size big enough to extract good amount of distinctive features [7].

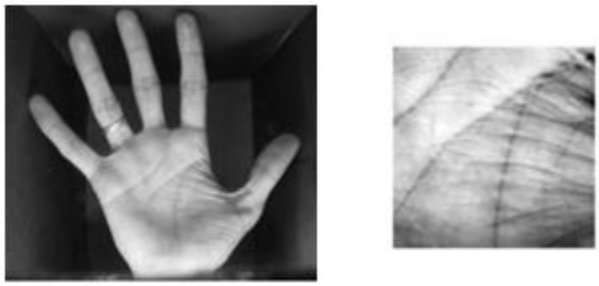

Fig. 1.6 Original palm image and its extracted ROI

After ROI extraction, distinctive features are extracted using suitable feature extraction technique and then this feature set is matched with another feature set to obtain matching score. The value of matching score then decides whether the person is authentic or not.

1.3.2 Knuckleprint

Knuckle is the joint present in the finger which helps the finger to bend forward. Through this bending forward action and resisting backward movement, a pattern of creases and wrinkles are formed on knuckles. These creases and wrinkles become permanent as we age. Thus, like palmprint, finger knuckle also contain line features which can be used as a biometric identifier.

Although less in number, they can be used in authentication purposes. Pattern formed at knuckles is unique and provides discriminating textural features. Finger knuckles have achieved less attention among researchers and not much work has been done on it for

authentication and recognition purposes.

The advantages of employing knuckle in biometric systems are numerous [17].

1. High user acceptance: Users are more willing to give outer palm surface for imaging than inner surface due to hygiene issues.

2. While imaging, one can also acquire finger geometry information which can be employed in improving authentication performance.

3. Knuckle features can also be taken using peg-free imaging system.

To employ knuckleprint in authentication techniques, following steps need to be taken.

1. Knuckleprint acquisition

2. Knuckle ROI extraction

3. Feature extraction

4. Feature matching

1. Knuckleprint acquisition: The acquisition device used to acquire knuckle print images includes tools namely finger bracket, a LED ring source, a lens, a CCD camera and a frame grabber as shown in figure 1.7 [9]. Finger bracket contains a triangular block and basal block which helps in keeping finger firmly during acquisition. Ring LED light source ensures good lightning conditions by concentrating light on the finger during image capturing. CCD camera captures the picture and transmits it to data processing module which further extracts ROI from it.

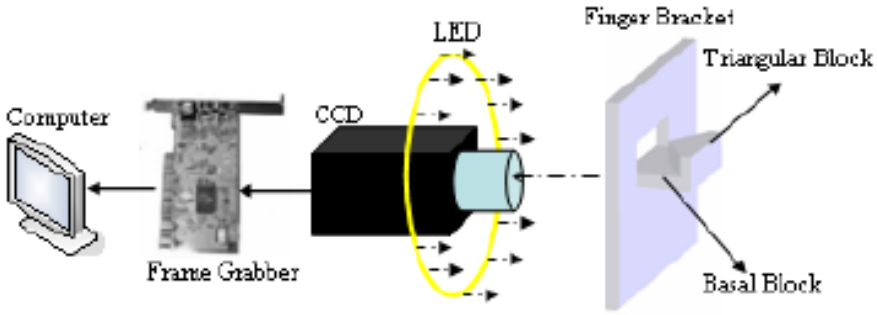

Fig. 1.7 Finger knuckle print acquisition device [9]

2. ROI extraction: The bottom boundary is extracted using canny-edge filter. This extracted boundary becomes the x-axis of the coordinate system. Further,canny edge detector is employed to obtain the edge map. Now from this edge map, y-axis is determined. In knuckles, curves are either convex leftwards or convex rightwards. This is estimated using convex direction coding. Pixels on convex leftwards curves are coded as 1, while those on rightwards are coded as -1. Pixels with no curves are coded as 0. After this is estimated, y-axis can be determined as curves exactly on the joint don't have any convex directions. Once x-axis and y-axis are fixed, ROI subimage can be extracted. Figure 1.8 shows ROI images of two knuckleprint images [9].

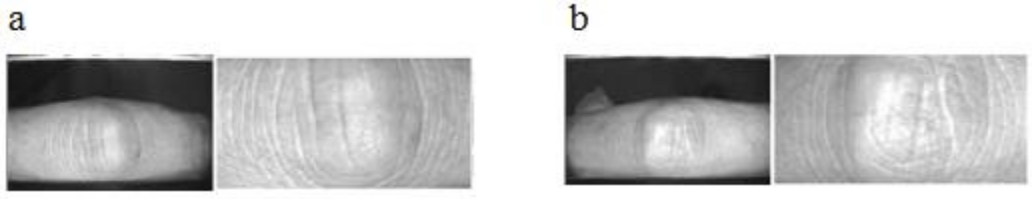

Fig. 1.8 ROI images of two knuckle images [9]

After the ROIs are extracted, textural features are extracted and matched using suitable matching strategy for authentication.

1.4 Thesis Objective and Scope

The main objective of this thesis is:

1. To find new approaches for line feature extraction for authentication purposes which can give better results than previous techniques.

2. To enhance the results of recognition while using line features of palmprint.

In order to achieve these goals, following are the sub-goals we acted upon:

1. What all traits are available for recognition purposes.

2. Determining the merits and demerits of all traits.

3. Identifying the various features associated with palmprint and knuckleprint.

4. Identifying the various feature extraction techniques which can be helpful for our work.

5. Implementation of feature extraction techniques on palmprint and knuckleprint.

Scope of this work is limited to identification and verification processes in biometric recognition systems.

1.5 Thesis Outline

The rest of the paper is organized as follows: In Chapter 2 we give a brief description of feature extraction and all the important papers and literature that we have studied or utilized as a part of our related work. In Chapter 3, we discuss the techniques used in this work for feature extraction and matching those feature sets. Chapter 4 explains in detail the proposed work and all the extensive experiments done. Chapter 5 illustrates and discusses the results obtained from the extensive experiments done using feature extraction approaches on all the databases. Chapter 6 outlines the conclusion and future work of this project.

Chapter 2
Feature extraction and Related work

2.1 Feature Extraction

Feature extraction stands for extracting features from a biometric image or ROI which can uniquely characterize/represent that particular image and can help in identifying an individual. After feature extraction, the vital information of the image gets stored in the compact form known as feature set. This feature set is matched using appropriate similarity measure for authentication purposes. Feature extraction is one of the most challenging and difficult step in authentication process.

Different modalities have their own features. Like in fingerprint, whorl, loops, delta are features at global level while at local level, minutiae points are considered as features. Minutiae points are points where the ridges on fingerprint are discontinuous. In palmprint, wrinkles, principal lines, ridges and texture are the main features. In knuckle print, pattern formed by bending of finger is very unique thus the curved lines and creases are considered as a feature for knuckle print. So depending on the type of features, different feature extraction techniques are employed.

After feature extraction, they are matched. A number of matching strategies are there to match feature sets namely Euclidean distance, cosine similarity, hamming distance, L norm, Manhattan distance etc. But not every matching strategy can work upon any feature set i.e. the matching strategy depends on the type of feature set. Like for binary encoded feature sets, hamming distance should be used.

There are many detectors available which can extract potential features from the images namely Scale Invariant Feature Transform (SIFT), HARRIS, Histogram of Gradients (HOG), Moravec corner detector etc. We have studied several feature detectors and understood their technique.

2.2 Related Work

Extraction techniques on palmprint are classified into 4 major classes: (1) texture based approach, (2) appearance based approach, (3) orientation based approach and (4) line based approach [16]. Salient features of these approaches are highlighted in table 1 [16]. In texture based approach, textural features are extracted from the normalized palm image. Other methods of textural based approach includes: Discrete cosine transform (DCT), Discrete Fourier transform (DFT) and wavelets transform [16]. Main technique in extracting textures is 2-D Gabor filter which has confirmed a satisfactory performance in palmprint authentication [7]. Appearance based approach is also known as subspace learning approach in the literature of palmprint recognition [18]. In this approach, subspace is build by learning from training data, and then unknown image is projected into this subspace. Some common methods in this approach are: Principal Component Analysis (PCA), Linear Discriminant Analysis (LDA). Then the similarity is measured using coefficients of training and unknown image. In orientation based approach, orientation of pixels are extracted and used as features to perform recognition. This approach is a very promising approach since orientation has a great distinguishing power in that it is rotation and illumination invariant [31]. In line based approach, principal lines and wrinkles are extracted for they are used as features to distinguish palm images.

Table 2.1 Classification of palmprint feature extraction approaches.

S. no.	Approach	Examples	References
1	Texture based	Gabor filter	[7]
		Laws mask	[19]
		DFT	[20]
		DCT	[21]
		Wavelets	[22]
2	Appearance based	PCA	[23]
		LDA	[24]
3	Orientation based	Competitive coding scheme	[28]
4	Line based	Phase congruency feature extraction	[29]
		Line matching	[25]
		Crease detection	[26]
		Morphological operators	[27]

Other related work on palmprint for recognition purposes includes:

Zhang and Zhang used wavelet expansion and context modeling techniques to retrieve principal lines from the palm image [8]. Han, Cheng, Lin and Fan proposed Sobel and morphological operations to extract the line features from palm images [9]. Also, Wang et al. and Liu et al. proposed some approaches for palm lines extraction [10-12]. Morales et al. have also done some significant work on contact less palmprint images [13]. Tee Connie et al. have given a robust approach on knuckle and palmprint recognition using contact-less databases [14]. Badrinath et al. used method Scale Invariant Feature Transform (SIFT) to extract features from constrained palmprint images [15].

Related work on radon transform and sparse representation for recognition purposes includes:

D. S. Huang et al. proposed modified finite Radon transform to extract principal lines from contact based palmprint database [31]. A. Kumar employed sparse representation technique in ear identification [32].

Chapter 3
Extraction and Matching Techniques

3.1 Gabor filter

The Gabor filter was originally introduced by Dennis Gabor in 1946 [1]. The 1-D Gabor filter is defined as the multiplication of a cosine/sine (even/odd) wave with a Gaussian windows defined as

$$g_e(x) = \frac{1}{\sqrt{2\pi}\sigma} e^{-\frac{x^2}{2\sigma^2}} \cos(2\pi u x) \tag{3.1}$$

$$g_o(x) = \frac{1}{\sqrt{2\pi}\sigma} e^{-\frac{x^2}{2\sigma^2}} \sin(2\pi u x) \tag{3.2}$$

where $g_e(x)$ represents even wave or cosine wave and $g_o(x)$ represents odd wave or sine wave, u is the frequency and σ the spread of the Gaussian window.

Thus the complex Gabor filter is given by

$$G(x) = g_e(x) + i g_o(x) \tag{3.3}$$

$$= \frac{1}{\sqrt{2\pi}\sigma} e^{-\frac{x^2}{2\sigma^2}} \left(\cos(2\pi u x) + i \sin(2\pi u x)\right) \tag{3.4}$$

$$= \frac{1}{\sqrt{2\pi}\sigma} e^{-\frac{x^2}{2\sigma^2}} e^{i(2\pi u x)} \tag{3.5}$$

Daugman in 1980 further extended the Gabor filter in two dimensions. Gabor filters are similar to Fourier filters but they are limited to certain frequency bands. Gabor filter can be used to extract textural details from an image.

David Zhang in 2003 proposed a 2D Gabor phase coding scheme for palmprint representation [1]. He used circular Gabor filter which is a great tool for textural features extraction. Circular Gabor filter is defined as

$$G(x, y, \theta, u, \sigma) = \frac{1}{2\pi\sigma^2} \exp\left\{-\frac{x^2 + y^2}{2\sigma^2}\right\} \exp\{2\pi i(\text{uxcos}\theta + \text{uysin}\theta)\} \tag{3.6}$$

Where $i=\sqrt{-1}$, u is the frequency of the sinusoidal wave, θ adjusts the orientation of the function and σ is the standard deviation of the Gaussian envelope.

Gabor 2D phase coding depends on values taken for the different parameters θ, u and σ.

It is to be noted that large value of σ makes the filter more robust to noise but it will extract more spurious features. Smaller value of σ makes the filter less effective. Thus a suitable σ has to be chosen to ensure effectiveness.

Figure 3.1 shows a palmprint image and its gabor filtered image.

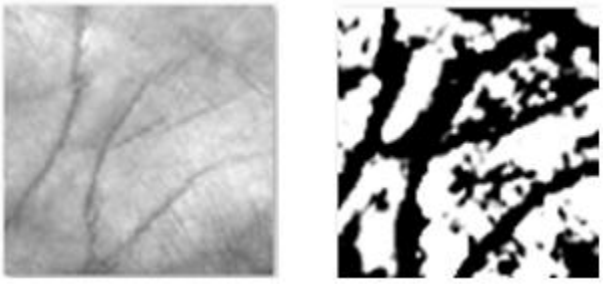

Fig. 3.1 Original palmprint and corresponding Gabor filtered palm image

3.2 Radon Transform

The Radon transform is named after the Austrian mathematician Johann Karl August Radon (December 16, 1887 – May 25, 1956) [30]. It was established in 1917 by Johann Karl august radon. Main application of radon transform is computer aided tomography (CAT) scans because major motivation of radon transform was CAT scans. In CAT

scans, a series of x-rays is passed through a person's body. Each ray gives us the information regarding the path it covers. The tissue it reaches is considered as the three dimensional space inside the body and rays gives the line integral function of this space. This method of retrieving line information from 3D space inside the body is known as continuous or finite radon transform.

The radon transform of a continuous two dimensional function *f (x, y)* is written as

$$R(\rho,\theta)[f(x,y)] = \int_{-\infty}^{\infty}\int_{-\infty}^{\infty} f(x,y)\delta(\rho - x\cos\theta - y\sin\theta)dxdy \tag{3.6}$$

where $\delta(\cdot)$ is a dirac delta function, ρ is the perpendicular distance of a line from the origin and θ is the angle between the line and the y-axis. Radon transform maps Cartesian coordinates (x, y) to polar coordinates (ρ, θ). Radon transform of the binary image is illustrated in figure 3.2.

Since this eq (3.6) spans the entire image to detect a line and thus is not useful for the detection of smaller line segments due to the infinity limit imposed on the integral. Thus to solve this problem, Copeland et al. proposed a new scheme for Radon transform known as Localized Radon transform [33] which is defined as

$$R(\rho,\theta)[f(x,y)] = \int_{x_{min}}^{x_{max}}\int_{y_{min}}^{y_{max}} f(x,y)\delta(\rho - x\cos\theta - y\sin\theta)dxdy \tag{3.7}$$

Where x_{max}, x_{min}, y_{max}, y_{min} are the parameters to describe a local area to perform Radon transform.

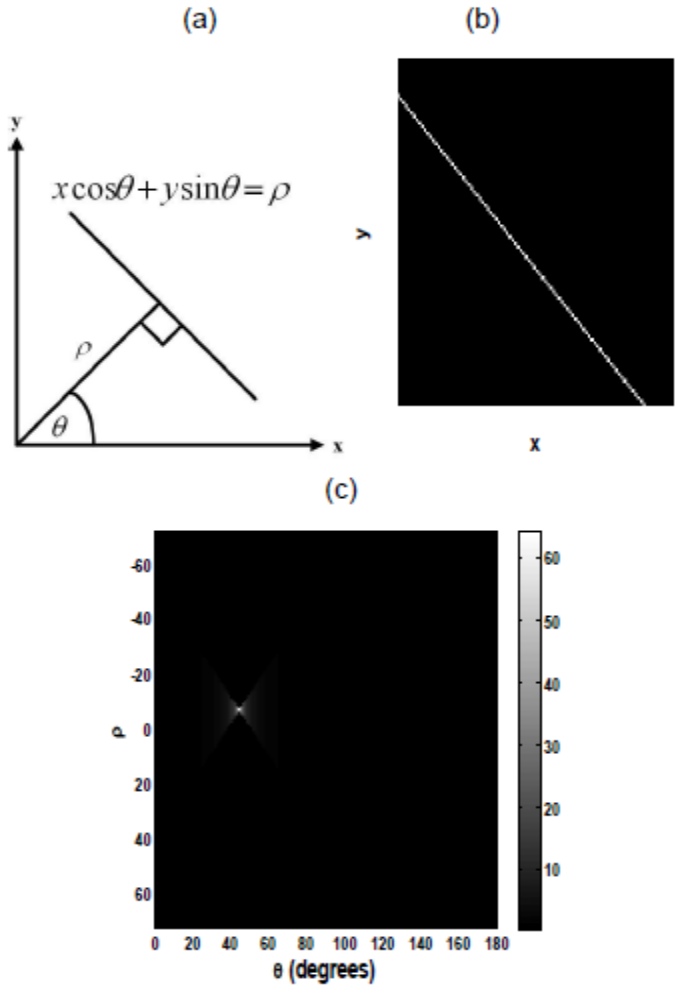

*Fig.3.2 (a**).** Parameters for Radon transform. (**b**) A binary image consist of a line **(c**) Radon transform of the binary image. The bright spot indicates the line in parameter domain [38].*

However if the signals are limited by some finite length, then the radon transform is known as finite radon transform (FRAT) [3]. FRAT helps in highlighting the line trends in the image by summing the intensity values of all the points on all the lines in the image.

Thus FRAT is defined as the summation of all image intensity values on a small set of lines in an image.

Feature extraction procedure using Radon transform

Let Z_p = [0, 1… p-1], where p is the prime number, FRAT on a 2D function f (x, y) on a finite grid Z^2p can be defined as:

$$r_m [c]=FRAT\, f(m, c) = \frac{1}{\sqrt{p}} \sum_{(i,j)\in Lm,c} f[i, j] \tag{3.8}$$

Where $L_{m,c}$ denotes the image pixels that make up a line on the grid Zp^2 which means:

$$L_{m,c} = \{ (i, j) : j = mi + c \ (\text{mod } p), \text{i} \in Z_p \}, 0 \leq m < p, \tag{3.9}$$

$$L_{p,c} = \{ (c, j) : j \in Z_p \}. \tag{3.10}$$

Where m is the corresponding slope of the line and c is the intercept.

In the equation 3 above, due to modulus operation, FRAT performs the "wrap-around" operation on the image again and again. So to eliminate or diminish this wrap-around effect, a more enhanced version of FRAT emerges known as modified finite radon transform (MFRAT) [31].

$$r[L_m] = MFRAT_f(m) = \frac{1}{C} \sum_{(i,j)\in Lm} f[i, j], \tag{3.11}$$

where C is the scale controller parameter of $r[L_m]$ and L_m represents the image pixels that make up a line on the grid Zp^2 , which means:

$$L_m = \{(i, j) \mid j = m (i - i_0) + j_0, i \in Z_p \}, \tag{3.12}$$

Where (i_0, j_0) represents the center pixel of the grid Zp^2, and m is the corresponding slope of L_m. Thus in this, summation of all pixels is done on the line which passes through the center pixel at slope m in the grid.

Using this technique of MFRAT, we can very easily compute the energy and the orientation of every pixel of the image. The orientation θ of the center pixel in the grid Zp^2 is computed as taking that orientation at which the $r[L_m]$ value is least in that grid. The orientation or angle can be computed using the slope m. Thus the slope at which $r[L_m]$ value is least, compute the orientation corresponding to that slope and set it as the orientation of the center pixel of that grid.

$$\begin{aligned} \theta_{m(i_0,\, j_0)} &= \arg(\min_m(r[L_m])), \quad m = 1,2,\ldots,N, \\ e_{(i_0,\, j_0)} &= \left|\min(r[L_m])\right|, \qquad\quad m = 1,2,\ldots,N \end{aligned} \tag{3.13}$$

Where $|.|$ represents absolute operation.

Since slope m is

$$m = \tan\theta$$

Thus calculating the $\tan^{-1}$ of this m will gives us the corresponding θ.

And energy of the central pixel is set as least value of $r[L_m]$ in the grid Zp^2.

We can calculate orientation θ and energy e of every pixel by shifting this grid through each row and column and thus can obtain an *Orientation_matrix* and *Energy_matrix* which gives a lot of information about the image. Let say image has dimensions u x v.

$$Orientation\_matrix = \begin{vmatrix} \theta_{m(1,1)} & \theta_{m(1,2)} & \vdots & \theta_{m(1,\, v)} \\ \theta_{m(2,1)} & \theta_{m(2,2)} & \vdots & \theta_{m(2,\, v)} \\ \cdots & \cdots & \cdots & \cdots \\ \theta_{m(u,1)} & \theta_{m(u,2)} & \vdots & \theta_{m(u,\, v)} \end{vmatrix} \tag{3.14}$$

$$energy\_matrix = \begin{vmatrix} e_{(1,1)} & e_{(1,2)} & \vdots & e_{(1,\, v)} \\ e_{(2,1)} & e_{(2,2)} & \vdots & e_{(2,\, v)} \\ \cdots & \cdots & \cdots & \cdots \\ e_{(u,1)} & e_{(u,2)} & \vdots & e_{(u,\, v)} \end{vmatrix} \tag{3.15}$$

Thus two new images can be obtained namely: *Orientation_image* and *Energy_image*.

Then from the *Energy_image*, important lines are extracted based on a threshold value *thresh.* Threshold value *thresh* is computed by first sorting *energy_matrix* in descending order and then selecting M^{th} largest pixel. Thus binary *Lines_image* can be defined as

$$Lines\_image(x,y)=\begin{cases}1 & \text{if Energy\_image}(x,y) < thresh. \\ 0 & \text{if Energy\_image}(x,y) \geq thresh.\end{cases} \quad (3.16)$$

In the *Lines_image*, only the principal lines and strong wrinkles get highlighted. It is worthy to note that directions of principal line differ from that of wrinkles. Now to separate principal lines from wrinkles, *LA_image* and *LB_image* are constructed in the following manner

LA_image(x, y) = 1 if *Lines_image(x, y)* = 1 and $0^0 < \theta_{(x,\,y)} \leq \pi/2$ (3.17)

LB_image(x, y) = 1 if *Lines_image(x, y)* = 1 and $\pi/2 \leq \theta_{(x,\,y)} < \pi$. (3.18)

Now to account for whether *LA_image* contains principal lines or *LB_image*, Radon energy maps are created which are *R[LA_image(x, y)]* and *R[LB_image(x, y)]* respectively. Since principal lines are darker and straighter than wrinkles, thus radon energy of principal lines will be greater than that of the wrinkles. Thus by comparing the energy of the two radon maps, we can determine which image has principal lines.

3.3 SPARSE REPRESENTATION

The concept of sparse representation has emerged from the field of statistical signal processing where the sparse representation is used with respect to signals atom. The prime purpose of sparse representation is to represent and compress the signals with the sampling rate much lower than that of Shannon Nyquist method. Sparse representation is widely used in many signal processing applications like noise reduction, compression, linear regression, transform coding etc. The underlying principal of sparse representation is to select a subset of features which can uniquely identify a signal from a set of signals [4, 5]. Sparse representation can be very well used in recognition and classification as

well [5].

Sparse representation helps in classification [5]. Sparse representation represents a sample with respect to a dictionary such that the representation is sparse and linear.

Given a test sample *y* from one of the classes in training set and a dictionary of training samples, sparse representation $\hat{y}$ of *y* over this dictionary can be computed. This $\hat{y}$ vector is a sparse vector with few non-zero entries. The training samples corresponding to these non-zero entries represent the class of test sample. Thus, we can easily assign that test sample to that class. However practically, due to the presence of noise, some non-zero entries may appear corresponding to other classes in the dictionary.

However, such heuristics doesn't work for images. So, to classify image sample *y,* we compute coefficients of all the training image samples of each class and see which class's coefficients best reproduce *y.*

The characteristic function δ_i selects coefficients associated with i_{th} class. So for *x,* δ_i (x) is a new vector whose only non-zero entries are the entries in *x* that are associated with the i_{th} class. Using these coefficients, one can reproduce *y* as

$$\hat{y}_i = D\delta_i(x) \tag{3.19}$$

Then *y* is classified to that class that minimizes the residual between *y* and $\hat{y}_i$.

$$\min_i r_i(y) = \left\| y - D\delta_i\left(\hat{x}_1\right) \right\|_2 \tag{3.20}$$

Thus the steps for classification are:

First of all, a dictionary D of training samples is computed for *k* classes' i.e.

$$D = [D_1, D_2, D_3 \ldots D_K] \in R^{m \times n} \tag{3.21}$$

Test sample *y* which is to be classified also belongs to R^m.

Then normalize the columns of D. After this, l1-optimization problem is solved using appropriate algorithm.

$$\hat{x}_i = \text{argmin}_x \left\| x \right\|_1 \text{ subject to } Dx=y \tag{3.22}$$

Then, residuals are computed for each class *k* as

$$r_i(y) = \left\| y - D\delta_i\left(\hat{x}_1\right) \right\|_2 \tag{3.23}$$

And based on the residuals we can identify the appropriate class of *y* as

$$\text{Identify}(y) = \text{argmin}_i \, r_i(y) \tag{3.24}$$

By this way sparse representation of images can be done.

3.4 Hamming Distance

Hamming distance was originally introduced in digital communication for error detection and correction. It was introduced by R. W. Hamming in 1950 [37]. It was introduced as the measure to determine the distance between two objects by counting the number of mismatches among the two corresponding variables. Here, in this work, it is used to calculate the difference between two feature binary vectors. It calculates the number of different bits between two bit vectors. Hamming distance is one of the widely used similarity measure in many applications to match two vectors.

For e.g. Hamming distance for two 4-bit strings are

(a) the Hamming distance of 0001 and 1100 is

$$D(0001, 1100) = 3.$$

(b) the Hamming distance of 1000 and 0001 is

$$D(1000, 0001) = 2.$$

Steps to calculate hamming distance are:

1. The two bit strings should be of equal length. The Hamming distance can only be calculated between two bit strings of equal length. Suppose String S1: "1001 0010 1000" and String S2: "1010 0010 0011".

2. Compare the first two bits in each string S1 and S2. If they are the same, record a "0" for that bit. If they are different, record a "1" for that bit. In this case, the first bit of both strings is "1," so record a "0" for the first bit.

3. Do step 2 for each bit in succession and record either "1" or "0" as appropriate. String S1: "1001 0010 1000" String S2: "1010 0010 0011" Record: "0011 0000 1011".

4. Add all the ones and zeros obtained in the record together to get the Hamming distance. Hamming distance = 0+0+1+1+0+0+0+0+1+0+1+1 = 5.

Chapter 4
Proposed Work & Experiments Done

4.1 Preview

A lot of work has been reported till date on palmprint but recognition using principal lines is very less. So, in this work, more emphasis is laid on extracting principal lines from palmprint than wrinkles since they are more stable and can't be concealed by bad lightning conditions. Many researchers claimed that principal lines can't be used as features due to their similarity among different individuals [7]. However, D. S. Haung et al. proved it wrong by discussing the discriminability of principal lines for recognition purposes [31].

4.2 Databases

We evaluated the below detailed approaches on two publicly available palmprint databases. The first database is Hong Kong Polytechnic University (PolyU) palmprint database [34]. This is the most widely used palmprint database in algorithmic researches. The PolyU palmprint database contains 2422 grayscale images in BMP format corresponding to 346 subjects. There are 7 samples from each subject. Size of the ROI image is 128 × 128. All the images were taken in constrained environment thus it is a contact-based database.

Second database used is touchless IITD palmprint database [35]. This database contains 1645 grayscale images in BMP format corresponding to 235 subjects. 7 samples were collected from each subject. Size of the ROI image is 150 × 150. Left hands are used for the palmprint acquisition. Acquisition method used for this database is peg-free thus resulting in contact-less images. Since the images were taken without any support, this database suffers from several drawbacks like rotational changes, translational changes

etc.

Third database used is Hong Kong Polytechnic University (PolyU) knuckleprint database [36]. This database has 4 datasets namely left index, left middle, right index and right middle. Each dataset has 1980 grayscale images in JPEG format obtained from 165 subjects including 125 males and 40 females. Each subject gave 12 samples. Size of ROI image is 220 × 110. Left index dataset has knuckle images obtained from left index finger. Same goes for other datasets. All the images were taken in unconstrained environment.

Before performing experiments, we created a Gabor enhanced database as well of PolyU palmprint database and IITD palmprint database. This database is created by applying Gabor filter to the images. Convolution of Gabor filter on the image enhances the textural features of image which helps in feature extraction. Thus all the experiments detailed below are performed on the original databases as well as Gabor enhanced databases. Performance is evaluated of each approach on original as well as Gabor enhanced databases. Parameter values used for Gabor filter are $\theta = \pi/4$, $\sigma = 5.6179$, $u = 0.0916$.

4.3 Experiments

Experiment 1:

Firstly Radon transform approach is employed to extract line features from palmprint databases.

Steps taken to implement this approach are:

1. Firstly, palm ROI images are normalized by computing mean of the image and then subtracting that mean value from each pixel of the image. Without this normalization step, all the further work would be ineffective.

2. Then MFRAT technique is employed which yields in *orientation_matrix* and *energy_matrix* of the normalized image. Grid size chosen for this approach is 14. Line width *w* is chosen as 2. Reason for choosing this grid size and line width is:

orientation_matrix size reduces to w^2, greatly decreases computation time and storage requirements also reduces due to reduced template size.

3. Then to compute the *lines_image*, *energy_matrix* is sorted in decreasing order and then threshold *thresh* value is empirically selected. Experiments are done taking different threshold values which range from 1000 to 1700. Performance obtained by setting different threshold values is being shown in figure 4.1 and 4.2. Figure 4.1 illustrates the performance for PolyU database image and figure 4.2 shows the performance for IITD database.

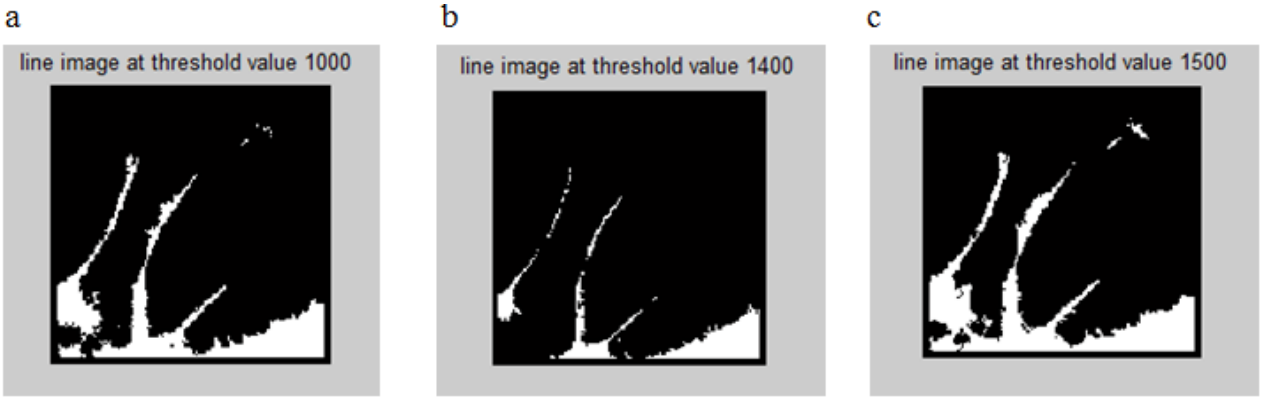

Fig. 4.1 Performance of computing lines_image at different threshold values for PolyU image.

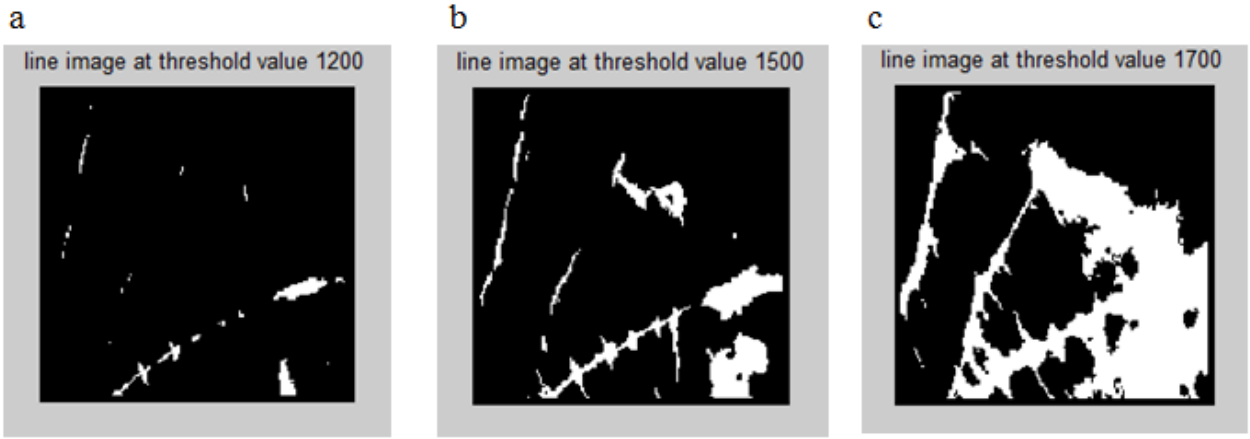

Fig. 4.2 Performance of computing lines_image at different threshold values for IIT D image.

Experiments done suggests thresh value of 1400 is best suited for PolyU database while for IITD database performance was best at thresh value of 1500. After the selection of suitable threshold value for each database, *lines_image* is generated by setting all those pixels from *energy_image* which has value greater than thresh value as 1 and rest remains 0.

4. After the *lines_image* is computed, *la_image* & *lb_image* are computed. *la_image* is computed for orientations from 15^0 to 90^0 while *lb_image* is computed for orientations which range between 90^0 to 180^0. However pixels with orientation 90^0 are kept in both the images.

5. Then Radon energy maps are plotted and it is observed that, in PolyU database, *la_image* corresponds to the image containing principal lines and *lb_image* comprises of wrinkles. Thus, principal lines have directions towards right side while wrinkles are more oriented towards left direction.

In IITD database, *la_image* corresponds to the image containing wrinkles and *lb_image* contains principal lines. Thus, principal lines have directions towards left side while wrinkles are more oriented towards right direction.

The resultant images obtained from the above steps for IITD database are shown in figure 4.3 and for PolyU database are shown in figure 4.4.

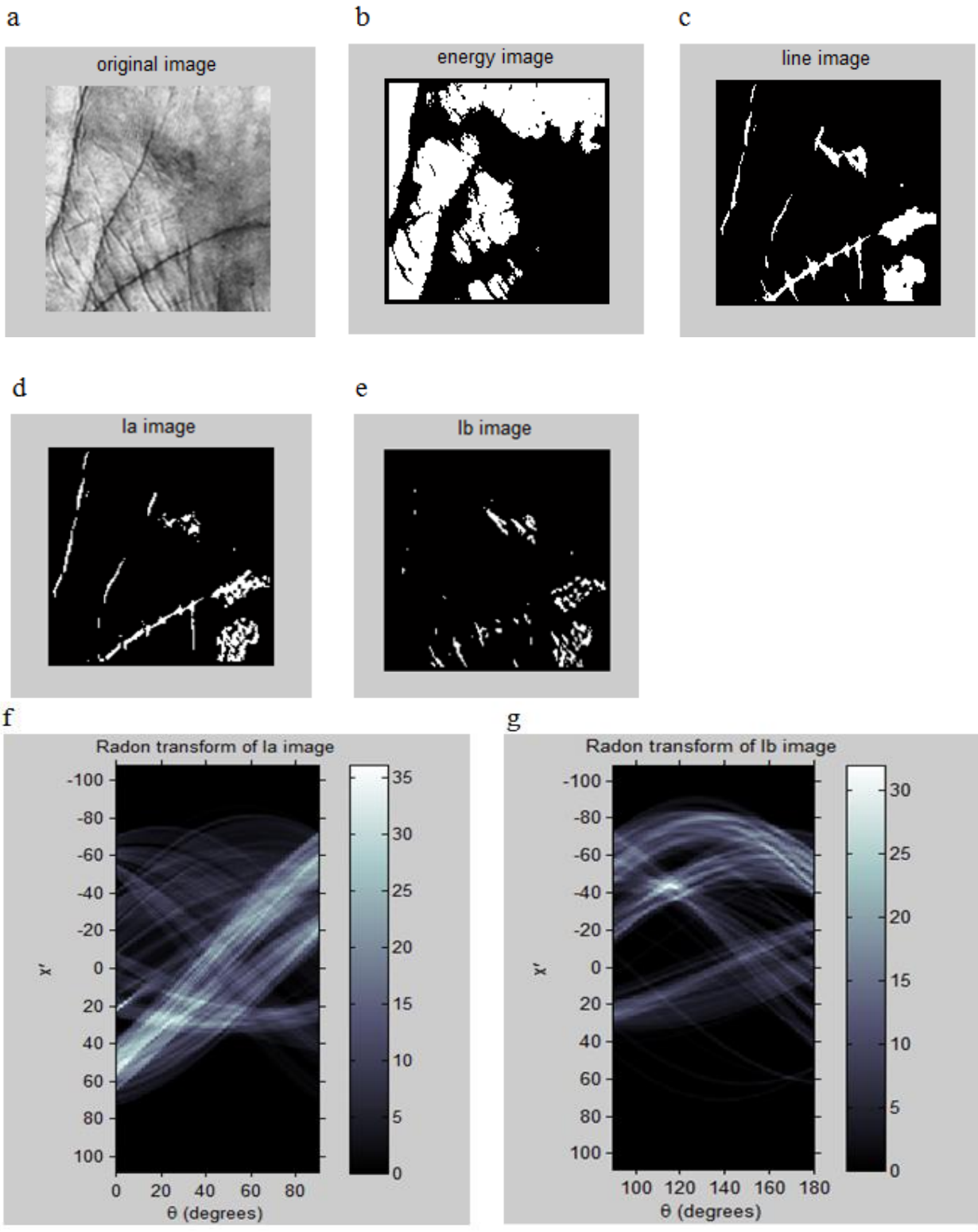

Fig. 4.3 Images of lines feature extraction using Radon transform. (a) Original image from IITD database; (b) Energy_image; (c) Lines_image; (d) LA_image; (e) LB_image; (f) R(LA_image); (g) R(LB_image).

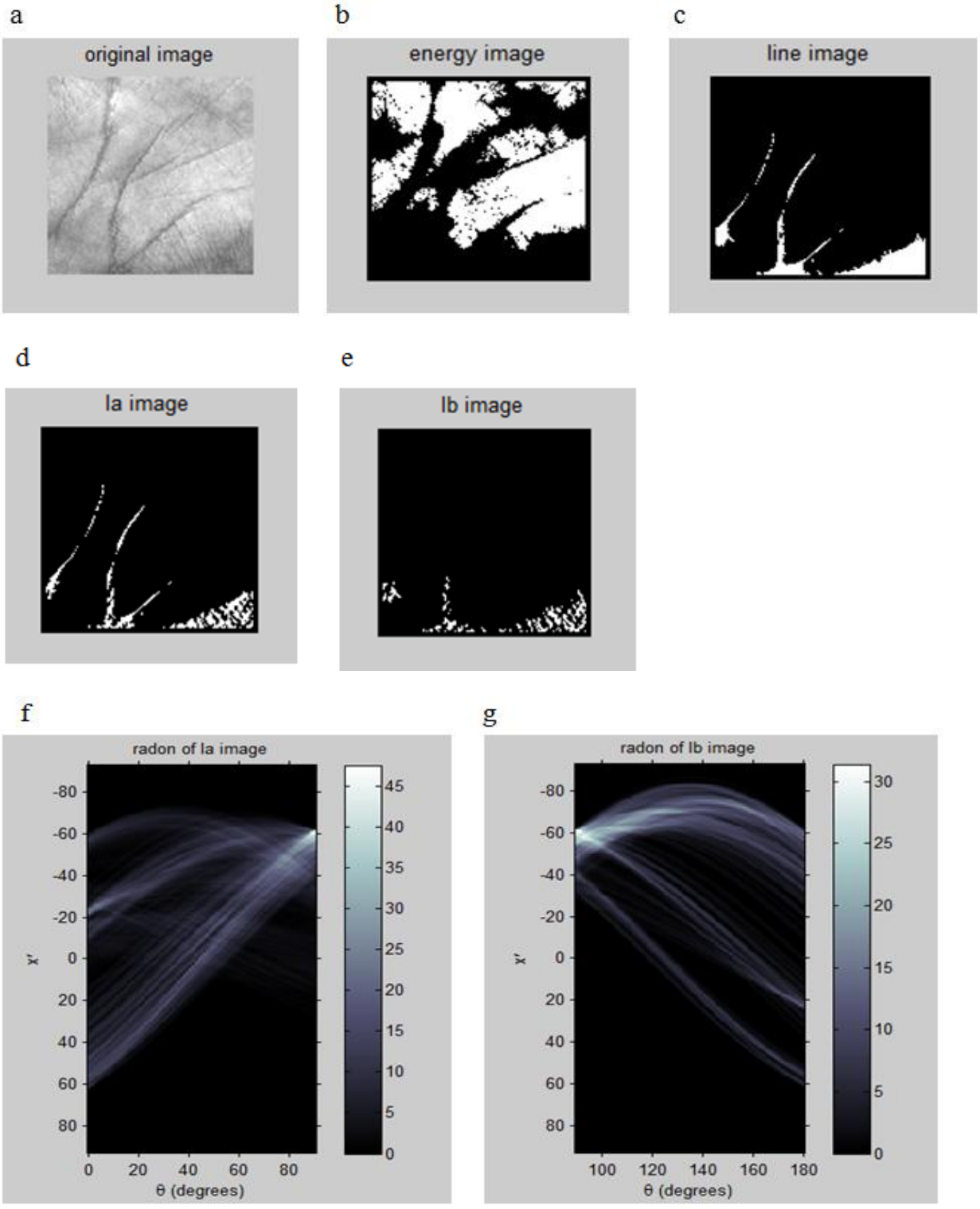

Fig. 4.4 images of lines feature extraction using Radon transform. (a) Original image from PolyU database; (b) Energy_image; (c) Lines_image; (d) LA_image; (e) LB_image; (f) R(LA_image); (g) R(LB_image).

From the above results, potential textural information about the image is carried in *orientation_matrix* and *energy_matrix*. Thus to measure the degree of similarity between two palmprints, Hamming distance is used as the similarity measure on *orientation_matrix* and the scores are recorded for genuine and imposter users on both the databases.

Experiment 2:

Keeping in mind the line features, a new approach is investigated namely sparse representation based localized feature extraction (S-LRT) [32] for line feature extraction utilizing the characteristics of both sparse representation technique which is computationally very efficient and radon transform which can extract line and textural features very well.

Steps taken in execution in S-LRT technique are:

1. Firstly all the ROI images are normalized.

2. Then a dictionary is designed in which each column represents a particular angle masks. These masks helps to retrieve the orientation information of dominanat lines in the images. Each column or element of the dictionary is defined as $[d^1 \ldots d^k]$ $R^{n \times k}$ where k<=n. The number of columns represent the number of angles taken into account for retrieving lines at those angles. These elements are constructed from a set of points S on a finite grid Zp^2 where $Z_p = [0, 1 \ldots p-1]$ and can be defined as:

$$S_\theta = \begin{Bmatrix} \{(x, y) \mid y = \tan\theta(x - x_0) + y_0, x \in Z_p\}, & \theta \neq \frac{\Pi}{2} \\ \{(x, y) \mid x = x_0, y \in Z_p\}, & \theta = \frac{\Pi}{2} \end{Bmatrix} \quad (4.1)$$

3. Image patches are taken from the normalized image, and its sparse representation i.e. coefficients $\alpha_{x,y}$ of each such patch $t_{x,y}$ (centered at (x, y)) is computed by solving the following l_1-regularized convex optimization problem:

$$\min_{\alpha_{x,y}} \left\| D\alpha_{x,y} - t_{x,y} \right\|_2^2 + \lambda \left\| \alpha_{x,y} \right\|_1 \tag{4.2}$$

4. This optimization problem is solved using fast iterative shrinkage thresholding algorithm (FISTA). The Lipchitz constant λ is experimentally selected and fixed as 0.02 for all experiments done.

5. All the resultant coefficients are observed and negative coefficients are clipped to zero and the index of the dominant orientation is binary encoded to extract the feature template.

6. All the above steps are repeated for every patch of the image thus covering every pixel. The resultant matrix is termed as feature template.

This feature template is constructed for every image. To match these feature templates for recognition, we have used Hamming distance as the matching strategy since this proves to be the best matching technique when it comes to binary encoded features.

These approaches are applied on both the palmprint databases and the genuine and imposter scores are recorded.

Experiment 3:

Seeing the performance of S-LRT, we also applied this approach on PolyU Knuckleprint database as well and the results are discussed in next chapter.

Chapter 5
Results & Discussions

5.1 Preview

The experimental results using the approaches detailed in the previous chapter are reported in this chapter. We performed these experiments with the four training and three test image samples on two publicly available palmprint databases namely: PolyU and IITD. We also performed some experiments on publicly available Knuckleprint database namely: PolyU database. In experimentation with this database, we took eight training and four test image samples.

For palmprint and knuckleprint authentication, performance is analyzed at FAR=0.01. We executed 3 set of experiments. First set of experiment includes application of MFRAT on palmprint databases. Second set of experiment includes application of S-LRT on palmprint databases. Third set of experiment includes application of S-LRT on knuckleprint database. Results are mentioned below experiment-wise.

5.2 Results

Experiment 1: Application of MFRAT on PolyU and IITD palmprint databases.

The results of application of MFRAT on cantact-based database i.e. PolyU database was GAR=69 at FAR =0.01. But the result drastically improved when gabor enhanced PolyU palmprint images were taken, resulting in GAR=95.5 at FAR=0.01. However, the results were not good on contact-less database i.e. IITD database giving GAR=33. Even the application of Gabor filter on IITD palmprint images could not helped in improving the results rather results got decreased on FAR=0.01 (GAR=31). However, on FAR=0.1, IITD database give GAR=38 and on Gabor enhanced IITD database GAR was 48. The ROC curve of PolyU palmprint database is shown in figure 5.1 and that of IITD

palmprint database is shown in figure 5.2. Red curve in the ROC plot is used for Gabor enhanced database while Blue curve denotes curve of original database.

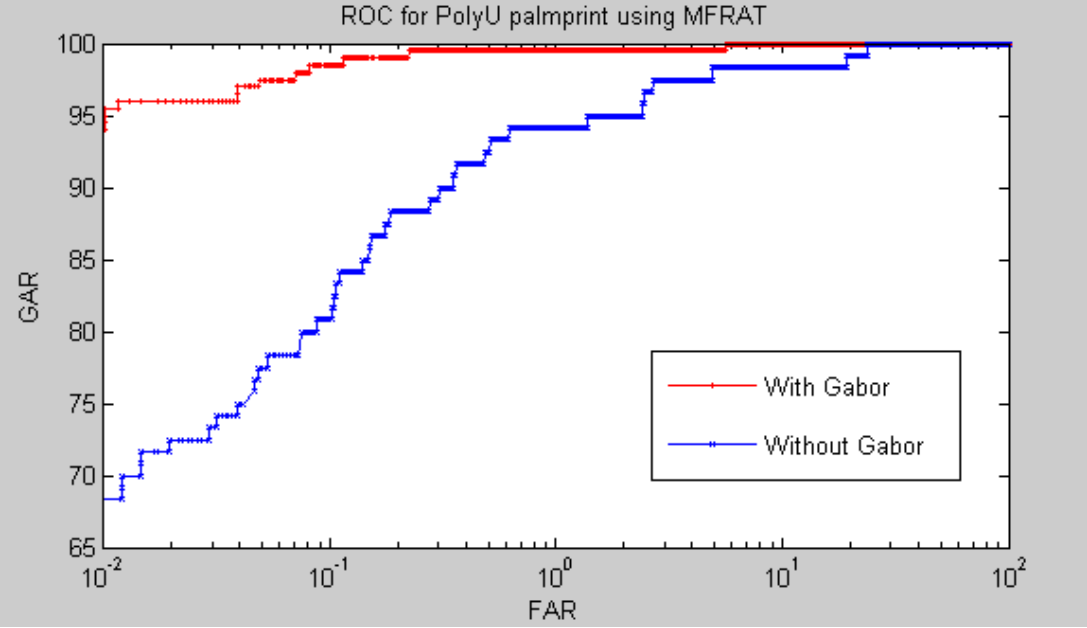

Fig. 5.1 ROC plot for PolyU palmprint database using MFRAT.

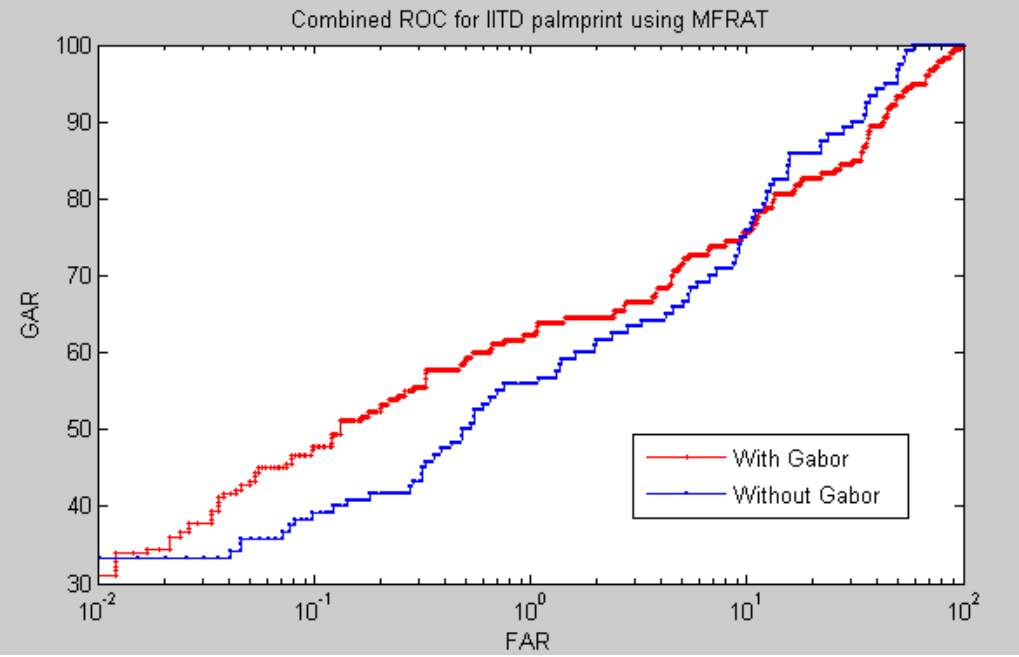

Fig. 5.2 ROC plot for IITD palmprint database using MFRAT.

Experiment 2: Application of S-LRT on PolyU and IITD palmprint databases

The results of application of S-LRT on cantact-based database i.e. PolyU database were good giving GAR=91.6 at FAR =0.01. And the result further improved when gabor enhanced PolyU palmprint images were taken, resulting in GAR=98.4 at FAR=0.01. However, the results were not good on contact-less database i.e. IITD database giving GAR=47. Even the applicaion of Gabor filter on IITD palmprint images could not helped in improving the results (GAR=55). The ROC curves for PolyU palmprint database is shown in figure 5.3 and for IITD palmprint database is shown in figure 5.4.

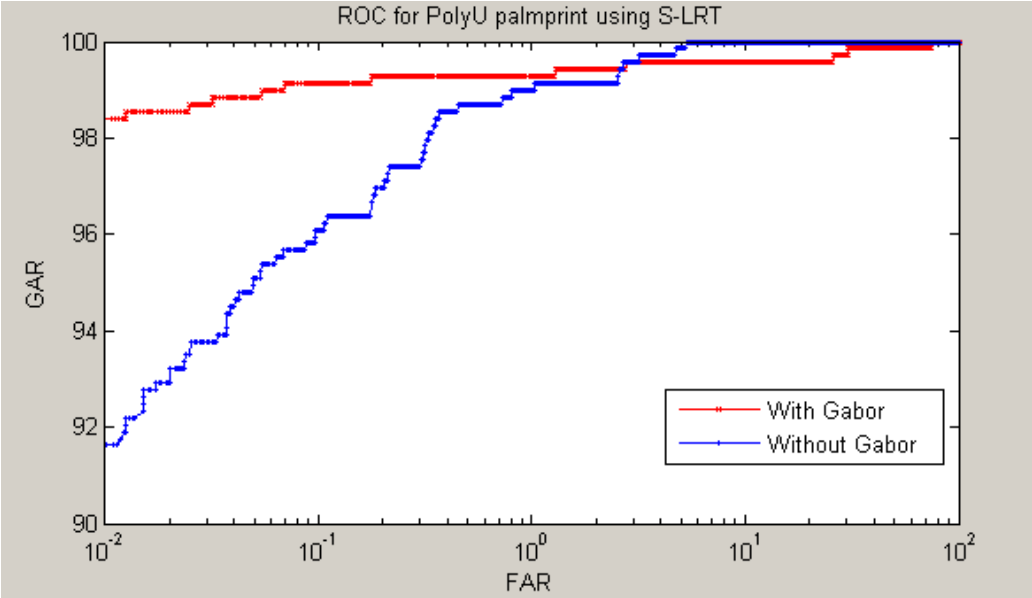

Fig. 5.3 ROC plot for PolyU palmprint database using S-LRT.

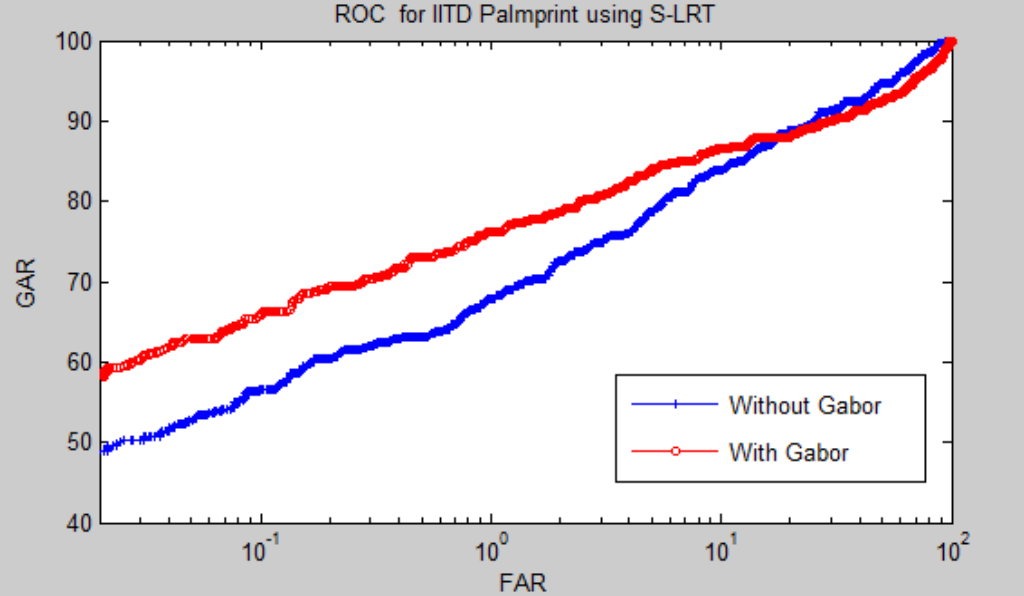

Fig. 5.4 ROC plot for IITD palmprint database using S-LRT

Experiment 3: Application of S-LRT on PolyU Knuckleprint database.

The experiments of S-LRT on PolyU Knuckleprint database is performed on 4 datasets namely left index dataset, right index dataset, left middle dataset and right middle dataset. Results of S-LRT on knuckle print database were low. GAR on left index dataset was 33 while on left middle it was 38. On right index dataset, GAR was 31 and on right middle, it was 46. Results on all the datasets are approximately same however it is worthy and interesting to note that performance on left middle and right middle is greater than on left index or right index. This shows that middle finger has more potential textural features than index finger. A combined ROC curve for all the PolyU knuckleprint datasets is shown in figure 5.5.

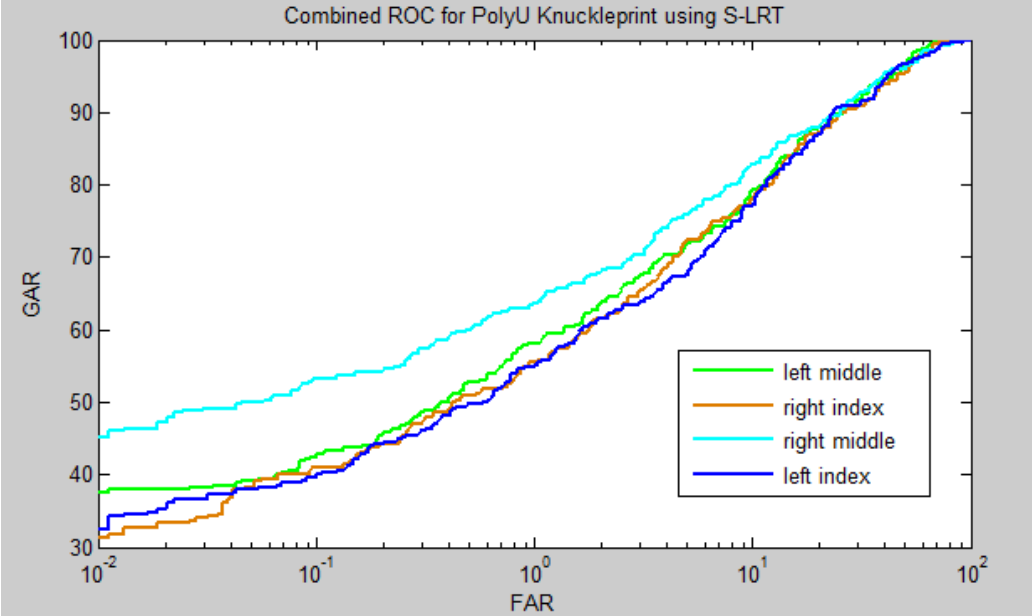

Fig. 5.5 Combines ROC plot for PolyU Knuckleprint database using S-LRT.

5.3 Summary of results

All the results observed from the above experiments are summarized in the following tables. And the best results are highlighted.

Table. 5.1 Performance of different approaches on PolyU palmprint database

Different Techniques	**With Gabor (WG)**			**Without Gabor (WOG)**		
	GAR(at FAR 0.01)	***GAR(at FAR 0.1)***	***GAR(at FAR 0.5)***	***GAR(at FAR 0.01)***	***GAR(at FAR 0.1)***	***GAR(at FAR 0.5)***
MFRAT	95.5	98.5	99.4	69	81	93
S-LRT	**98.4**	**99.2**	**99.4**	92	96.1	98.8

Table. 5.2 Performance of different approaches on IITD palmprint database

Different Techniques	**With Gabor (WG)**			**Without Gabor (WOG)**		
	GAR(at FAR 0.01)	***GAR(at FAR 0.1)***	***GAR(at FAR 0.5)***	***GAR(at FAR 0.01)***	***GAR(at FAR 0.1)***	***GAR(at FAR 0.5)***
MFRAT	31	48	60	33	38	48
S-LRT	55	66	74	47	58	64

Table. 5.3 Performance of S-LRT approach on PolyU knuckleprint database .

Dataset Used	***Gar(at far 0.01)***	***Gar(at far 0.1)***	***GAR(at far 0.2)***	***Gar(at far 0.5)***
Left index	33	40	45	50
Left middle	38	43	47	53
Right index	31	40	44	51
Right middle	46	54	55	60

5.4 Discussion

Here the effort was made to utilize the sparse representation of textural features of palmprint while Gabor filter is used as a baseline approach to enhance textural features in the image. This technique used the idea of extracting orientation information using localized radon transform technique. The significance of using MFRAT technique is its ease and simplicity of computation. Also by setting certain parameters like line width and grid size, we can greatly reduce the feature template size, which makes the technique much faster and thus efficient enough to be used in real life applications. On every database, S-LRT has always outperforms MFRAT.

Chapter 6
Conclusion

We successfully experimented the task of extracting line features from the palmprint databases using MFRAT and S-LRT approaches. The approach of S-LRT uniquely identifies orientation information from palmprint databse and thus gives best results with polyu palmprint database of 346 users. The best accuracy in the ROC plot was observed in the range 95 to 99 which seems quite satisfactory. The S-LRT approach perfomed much better than MFRAT approach on both the palmprint databases. And use of Gabor filter further enhances the results. The results of S-LRT on PolyU knuckleprint database confirms that middle finger has more potential features than on index finger. S-LRT gave satisfactory performance in principal line extraction thus making it useful in real applications of identification. Although S-LRT performed satisfactorily on contact based database, however it could not dealt with rotational and translational changes in the contact less IITD database that well. Thus it opens challenges in further research and developments to bring good results in case of contact-based database as well.

Future work of this project involves the experimentation and improvement of results of S-LRT approach on contact less databases as well as on images suffered from occlusion. For the refinement of results, different matching strategies can also be used that can deal with rotational and translational changes of images. The refinement should be such that it will be used in real applications.

References

[1] K. G. Derpanis, “Gabor filters”, York University, April, 2007.

[2] A.K. Jain, A. Ross, S. Prabhakar, “An introduction to biometric recognition”, IEEE Transactions on Circuits and Systems for Video Technology, vol. 14, no. 1, January 2004.

[3] F. Matus, J. Flusser, “Image representations via, finite radon transform”, IEEE transactions on Pattern Analysis and Machine Learning, vol.15, no. 10, pp. 996-1006, October, 1993.

[4] R. Raghavendra, “Sparse representation for accurate person recognition using hand vein biometrics”, Eighth International Conference on Intelligent Information Hiding and Multimedia Signal Processing, pp. 41-44, 2012.

[5] J. Wright, A. Y. Yang, A. Ganesh, S. S. Sastry, and Yi Ma, “Robust Face Recognition via Sparse representation”, IEEE Transactions on Pattern analysis and Machine Intelligence, vol. 31, no. 2, pp. 1-18, February 2009.

[6] W. Shu, D. Zhang, “Automated personal identification by palmprint”, SPIE Digital Library Opt. Eng. vol. 37, no. 8, pp. 2359-2362, Aug 01, 1998.

[7] D. Zhang, W. K. Kong, J. You, “On-Line Palmprint Identification”, Pattern Analysis and Machine Intelligence, IEEE, vol.25, no. 9, pp. 1041-1050, September, 2003.

[8] L. Zhang, D. Zhang, “Characterization of palmprints by wavelet signatures via directional context modeling”, IEEE Trans. Syst. Man Cybern. B., vol. 34, no. 3, pp. 1335-1347, 2004.

[9] L. Zhang, L. Zhang, D. Zhang, “Finger-knuckle-print: A new biometric identifier”, Image Processing (ICIP), IEEE, pp. 1981-1984, 2009.

[10] X.Q. Wu, D. Zhang, K. Q. Wang, B. Haung, " Palmprint classification using principal lines", Pattern Recognition, vol. 37, no. 10, pp. 1987-1998, 2004.

[11] X.Q. Wu, D. Zhang, K. Q. Wang, "Palm line extraction and matching for personal authentication", IEEE Trans. Syst. Man Cybern. A, vol. 36, no. 5, pp. 978-987, 2006.

[12] L. Lui, D. Zhang, "A novel palm-line detector", in: Proceedings of the 5th AVBPA, 2005, pp. 563-571.

[13] A. Morales, M.A. Ferrer and A. Kumar, "Towards contact-less palmprint authentication", IET Computer Vision, vol. 5, no. 6, pp. 407–416, 2011.

[14] G. Michael, T. Connie and A. Jin, "Robust Palm Print and Knuckle Print Recognition System Using a Contact-less Approach", 5th IEEE Conference on Industrial Electronics and Applications, pp. 323-329, 2010.

[15] G. Badrinath and P. Gupta , " Palmprint Verification using SIFT features", In Proceedings of International workshop on Image Processing Theory, Tools and Applications (IPTA), pp. 1-8, November, 2008.

[16] A. Kumar, D. Zhang, "Personal authentication using multiple palmprint representation", Pattern Recognition, vol. 38, pp. 1695 – 1704, 2005.

[17] A. Kumar, Y. Zhou, "Personal Identification using Finger Knuckle Orientation Features", Electronics Letters, vol. 45, no. 20, September 2009.

[18] K. Vaidehi, T. S. Subashini V. Ramalingam, S. Palanivel, M. Kalaimani, "Transform based approaches for Palmprint Identification", International Journal of Computer Applications (0975 – 8887), vol. 41, no.1, March 2012.

[19] J. You, W. Li, D. Zhang,"Hierarchical palmprint identification via multiple feature extraction", Pattern Recognition, vol. 35, pp. 847–859, 2002.

[20] W. Li, D. Zhang, Z. Xu, “Palmprint identification by Fourier transform”, Int. J. Pattern Recognition & Artificial Intelligence, vol. 16, no. 4, pp. 417–432, 2002.

[21] A. Kumar, D. Zhang, “Integrating shape and texture for hand verification”, in: Proceedings of the International Conference on Image & Graphics, ICIG 2004, Hong Kong, pp. 222–225, December 2004.

[22] A. Kumar, H.C. Shen, “Recognition of palmprints using wavelet-based features”, in: Proceedings of the International Conference on Systems, Cybern, SCI-2002, Orlando, Florida, July 2002.

[23] G. Lu, D. Zhang, K. Wang, “Palmprint recognition using eigenpalm-like features”, Pattern Recognition Letter, vol. 24, pp.1473–1477, 2003.

[24] X. Lu, D. Zhang, K. Wang, “Fisherpalms based palmprint recognition”, Pattern Recognition Letter, vol. 24, pp. 2829–2838, 2003.

[25] D. Zhang, W. Shu, “Two novel characteristics in palmprint verification: datum point invariance and line feature matching”, Pattern Recognition, vol. 32, no. 4, pp. 691–702, 1999.

[26] J. Funada, N. Ohta, M. Mizoguchi, T. Temma, K. Nakanishi, A. Murai, T. Sugiuchi, T. Wakabayashi, Y. Yamada, “Feature extraction method for palmprint considering elimination of creases”, Proceedings of the 14th International Conference on Pattern Recognition, vol. 2, pp. 1849–1854, August 1998.

[27] C.C. Han, H.L. Cheng, C.L. Lin, K.C. Fan, “Personal authentication using palm-print features”, Pattern Recognition, vol. 36, pp. 371–381, 2003.

[28] A. Kong, D. Zhang, “Competitive coding scheme for palmprint verification”, in: Proceedings of the 17th ICPR, vol. 1, pp. 520-523, 2004.

[29] J. Malik, R. Dahiya, G. Sainarayanan, "Personal authentication using palmprint with phase congruency feature extraction", Image processing and Pattern recognition, vol. 4, no.3, September, 2011

[30] Wikipedia. Johann Radon. http://en.wikipedia.org/wiki/Johann Radon.

[31] D. S. Huang, W. Jia, D. Zhang, "Palmprint verification based on principal lines", Pattern Recognition, vol. 41, pp. 1316 – 1328, 2008.

[32] A. Kumar, T. S. T. Chan, "Robust ear identification using sparse representation of local texture descriptors", Pattern Recognition, vol. 46, pp. 73–85, 2013.

[33] A. C. Copeland, G. Ravichandran, M. M. Trivedi, "Localized radon transform-based detection of ship wakes in SAR images", IEEE trans. Geosci. Remote Sensing, vol. 33, no. 1, pp. 35-45, 1995.

[34] http://www4.comp.polyu.edu.hk/~biometrics/2D_3D_Palmprint.htm

[35] http://www4.comp.polyu.edu.hk/~csajaykr/IITD/Database_Palm.htm

[36] http://www4.comp.polyu.edu.hk/~biometrics/FKP.htm

[37] R. W. Hamming, "Error detecting and error correcting codes", Bell System Technical Journal, vol. 26, no. 2, pp. 147-160, 1950.

[38] A. Mostayed and S. Kim, "A peg free hand shape authentication scheme with radon transform", International Journal of the Physical Sciences, Vol. 6, no. 27, pp. 6303-6314, 2 November, 2011